Numerical modelling of deformation prediction for laser-assisted laser peen forming

Mingsheng Luo, Yongxiang Hu
[a] State Key Laboratory of Mechanical System and Vibration, School of Mechanical Engineering, Shanghai Jiao Tong University, China, huyx@sjtu.edu.cn

Keywords: laser peen forming, laser-assisted, numerical modelling.

Introduction

Laser peen forming (LPF) is a forming technique using laser-induced plasma to impact the workpiece spot-by-spot and forming the metal sheet into a specified curvature. It is a complex physics process including laser ablation, shock wave propagation, material yielding and deformation accumulation. A high-intensity short-pulsed laser irradiates on the surface of the workpiece, as a result, high pressure plasma generates on the surface of the workpiece in the confinement of water. In the impact of high pressure plasma, the shock pressure generates and spreads to the depth direction. The amplitude of the shock wave arrives at 1-10 GPa and the time duration is around 100 nanoseconds, as a consequence LPF is a high-dynamic response process due to the laser shock process. When the shock wave exceeds the Von Mises stress of materials, the workpiece in the shock zone yields and generates plastic strain. After laser scanning over the workpiece surface, the deformation is accumulated with the expanding of the plastic zone, resulting in the workpiece bending into a small curvature convex shape. In order to overcome the difficulty of improving the pulse energy, laser-assisted laser peen forming(LALPF) was proposed by Hu et al. [1] to improve the bending capability. LALPF adapted CW laser heating to increase the deformation. Laser heating plays an assisted role in softening the material and altering the stress state of material during LALPF. Simutationly, the back surface of the workpiece is heating by continuous wave (CW) laser which is coaxial with the pulsed laser. The material absorbs the CW laser energy resulting in high temperature field in the local area. The local high temperature decreases the yield strength, inducing thermal stress even plastic thermal strain owing to the nonuniform expansion of material. Thus, lager and deeper plastic strain is generated in the laser shock process and the deformation of the workpiece increase compared with the LPF in room temperature.

The coupled thermo-mechanical mechanism in LALPF cannot be observed through experiment directly, therefore it is necessary and effective to use finite element method (FEM) to predict the bending of the workpiece in LALPF. However, this hybrid process of the continuous laser heating and noncontinuous of laser shock peening results in high computation cost because of the unmatch of the time scale in fully coupled thermo-mechancal numerical model. The time scale of single laser shock in LALPF is nanosecond in the discontinuous laser shock, while the time scale of the heating process is second in the continuous laser heating process, which results in huge computation during the simulation of fully coupled method. Therefore, the fully coupled method is not suitable for multi-time scale simulation of LALPF. To reduce computation costs, the sequentially coupled method simulates the two process dividedly: the temperature of laser heating is first simulated and then treated as the initial condition of following model. This method is used in many laser assist heating process, such as laser-assisted single point incremental forming [2], laser-assisted micro-milling [3]. Unlike these processes, LALPF is the characterized by extremely high shock pressure and short shock time, and the laser heating not only soften the material strength by increasing the temperature, but also may have an influence on the stress wave propagation due to superimposed stresses, which affects the plastic strain and finial deformation in the workpiece after laser shock. Furthermore, different from the common laser heating process, the water in LALPF worked as confined layer relatively moving on the surface of the workpiece during laser heating makes sequentially coupled FEM is more difficult to build.

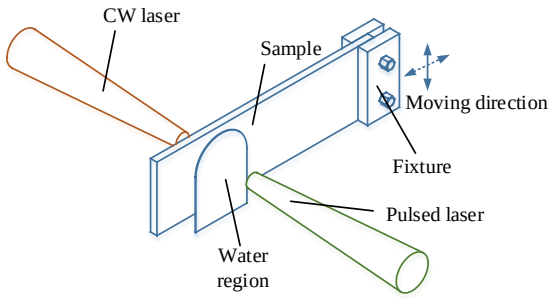

Fig. 1 The schematic of LALPF

Objectives

This paper presents a sequentially thermo-mechanical coupled numerical model of LALPF of Ti6Al4V sheet to predict the bending geometry and analyze the mechanism of capability improvement.

Methodology

LALPF finite model is developed to predict the deformation of the workpiece of Ti6Al4V. The dynamic laser heating influence the temperature field, thermal stress and thermal plastic strain, both of them have great influence on the plastic strain of laser shock, which causes the thermo-mechanical coupled effect. Considering time consuming of fully coupled thermo-mechancial model of LALPF due to the the unmatch time scale of the two process, the sequentially coupled model is used to simulated the thermal-mechanical coupled process of LALPF by dividing the two process separately and exported the temperature field as the initial condition of the model of LPF. However, the model of LPF is also hard to developed because the process is achieved by applying hundreds of high-dynamic laser shocks which is extremely time consuming to model the whole process explicitly. The eigenstrain model is proposed to prediction the deformation of LPF, where the eigenstrain in the eigenstrain model is derived from a small dynamic model of laser shock, which can greatly decrease the time of model of LPF. The FEM of LALPF is carried by commercial software ABAQUS, and the procedure is summarized as following: thermo-elastic-plastic model of laser heating is firstly simulated to gain the temperature field, thermal stress and thermal plastic strain; then the dynamic model of laser shock is carried out sequentially with the initial condition from the thermo-elastic-plastic model of laser heating; finally, eigenstrain method is used to predict the deformation of LALPF with the eigenstrain strain derived from the dynamic model. The flow chart of the modeling can be seen in **Fig. 2**.

The thermo-elastic-plastic model of laser heating is carried out to predect the temperaure, thermal stress and thermal plastic strain by a coupled temperature-displacement transient analysis step in

Fig. 2 The flow chart of the FEM for LALPF

ABAQUS. The material of workpiece is Ti6Al4V with the thickness of 2 mm and the size of 68 × 20 mm^2. The thermal flux of laser heating, defined by ABAQUS subroutine DFLUX, is a Gaussian distribution [4]. The continuous wave (CW) fiber laser with the wavelength of 1070 nm irradiate target surface is used to heating the workpiece with the desired beam diameter of 1.6 mm, and the absorptivity of CW laser is set 0.31 [5]. Scanning velocity V_y for CW laser is 10 mm/s, and the scan area is 40 × 20 mm^2 in the center of workpiece. The effect of water confinement must be taken into consideration in the thermal model because it has great effect on the temperature, and this effect is considered by setting the surface conviction boundary on the water covering area through ABAQUS subroutine FILM. The water covering area is assumed to be a shape of the reverse U shape, and the upper semicircle of the cooling zone is coaxial with the laser beam as moving relatively to the workpiece. The convection coefficient was 1968 $W/(m^2 \cdot K)$ for water convection boundary and the convection coefficient was 2.8 $W/(m^2 \cdot K)$ for the air convection boundary. The element type is C3D8RT (continuum, three-dimensional, 8-node reduced integration temperature element) with the size of 0.1×0.1×0.1 μm^3 in the scan line. The thermo-mechanical properties of Ti6Al4V is sensitive to the temperature, so, temperature-dependent material properties are utilized in the numerical model to reflect the effect of temperature on the mechanical behavior of laser peening during laser heating, such as thermal conductivity [6], specific heat [6] and Young's modulus [7]. The Johnson-Cook model [8] of Ti6Al4V is used in the thermo-elastic-plastic model and dynamic model.

The dynamic model is conducted by explicit code of to capture the dynamic response of laser shock [9] to determine the eigenstrain. The 3 × 3 arrays of laser shocks are carried out on the small-scale plate with the dimension of 6 × 6 × 2 mm^3 to take the overlap effect into account. The initial condition of the dynamic model is derived from the represent cell of the thermo-elastic-plastic model when the laser is heating the center point. The initial condition of every shock in the dynamic model should be the same, however the temperature field, thermal stress field and thermal plastic strain field of the 3×3 shocks couldn't keep the same when they are overlaps with each other. So, the average value of every layer elements in the represent cell is calculated and exported to the dynamic model as the initial condition. The infinite element (8-node 3-D solid continuum infinite element, CIN3D8) is used on four sides representing the rest of the workpiece to avoid the reflection of the stress wave. The other region is the finite element mesh (8-node 3-D solid continuum reduced temperature element, C3D8RT) with the size of 0.1×0.1×0.1 mm^3, which is fine enough to predict the high-dynamic process in the laser shock progress. The artificial damping [10] is used to reduce the duration time to guarantee the plastic strain filed in the saturated state. The space time between each shock is 1.0 μs to reduce the computation time. The pressure of laser shock is usually simplified as a Gauss distribution [11], and the time profile of the pressure is calculated by a one-dimension analytical model of confined plasma by Berthe et al. [12]. The maximum of the pressure is 3.70 GPa with 0.75 joule per shock. The distance of adjacent spot centers is 1.0 mm in the model.

The eigenstrain model is carried out by applying a unit temperature with the anisotropic thermal expansion ratios equal to the value of eigenstrain to predict the deformation and residual stress of workpiece. The eigenstrain indicates any strain arising in the material due to inelastic processes such as plastic deformation, thermal expansion and crystallographic transformation. In the eigenstrain model the eigenstrain is plastic strain derived from the represent cell of the dynamic mode. The shell element (S4R, 4-node general-purpose shell) with twenty-layer is used in the eigenstrain model. As the eigenstrain model is insensitive to the model size, the size of the element is 0.4 × 0.4 mm^2 and the number of the elements is 8500.

Results and analysis

Fig. 3 shows the result of thermo-elastic-plastic model of laser heating, dynamic model and eigenstrain model. The temperature, thermal stress and thermal plastic strain are derived from the

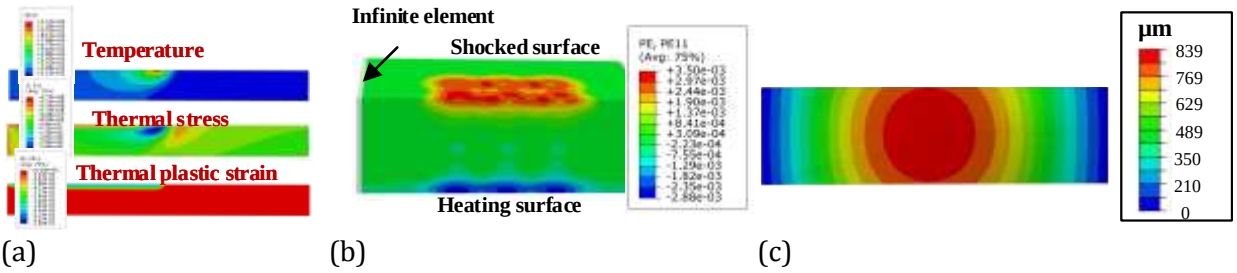

Fig. 3 Results of FEM for LALPF: (a) the temperature field, stress and plastic strain in the thermo-elastic-plastic model of laser heating, (b) the plastic strain in the dynamic model for LALPF, and (c) the prediction of deformation by eigenstrain model.

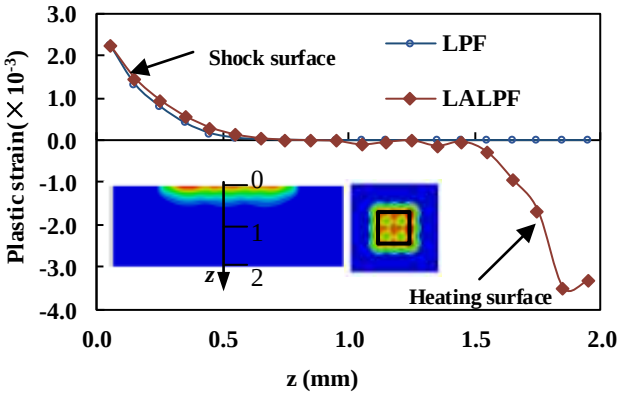

Fig. 4 The plastic strain in the dynamic model of LALPF and LPF under the pulse laser power density of 3.7 GW/cm^2 and the CW laser power of 142 W: the plastic strain in the z direction by averaging in the represent cell.

thermo-elastic-plastic model of laser heating to export into the dynamic model to gain the eigenstrain. The profile from eigenstrain model is derived to compare with the result of experiment..

show the plastic stain in the dynamic model of LALPF. According to the eigenstrain methodology [9], the plastic strain due to laser pen forming and laser heating determines the deformation of the workpiece. So the effect of laser heating of Ti6Al4V can be illustrated by the plastic strain in the dynamic model. The plastic strain in the dynamic model is the averaged in the represented cell of 2 × 2 mm^2, and the curve of plastic strain is plotted in.

. It can be seen that the plastic strain of LALPF is higher than the plastic strain of LPF in the shock surface and lower than the plastic strain of LPF in the heating surface. The plastic strain in the heating surface is negative, which can contribute to the bending of the workpiece according to the calculation of bending moment. So the laser heating results in the increase of plastic strain in the shock surface and generation of negative plastic strain in the heating surface, which is the main reason of improving the bending ability of LALPF.

Fig. 5 shows the deformation of the workpiece of LALPF versus the CW laser power. It can be seen that the arc height of workpiece increase with the CW laser power. The power of CW laser influence the how quickly the increase of arc height: when the laser heating power is low, the increase of workpiece increase slow; however when the laser power is high, the increase is faster. This is because the plastic strain of laser heating. When, the power of CW laser heating is low, the temperature is low, laser heating only induce the local high temperature field and thermal stress. When the power of CW

laser is high, laser heating induces local high temperature field, thermal stress and thermal plastic strain, which greatly increase the deformation of the workpiece. Especially the thermal plastic strain, which is negative plastic strain in the back of workpiece, contributes the moment for bending the workpiece.

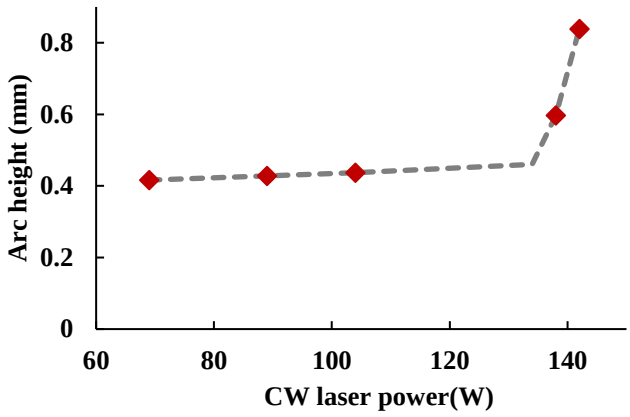

Fig. 5 The deformation of workpiece with the CW lase power.

Conclusions

This paper developed a FEM model for LALPF to study the deformation of workpiece in difference heating laser power. From the result of FEM, it can be concluded that:

1. The numerical model of LALPF is developed to predict the deformation of workpiece by sequence thermo-mechanically coupled model. The laser heating inducing high temperature field, thermal stress, thermal plastic strain, both of which have exported into the dynamic model and influence the dynamic process of laser shock and the finally deformation.
2. The influence of laser heating on the deformation can explained as reason of the increase of deformation. When the CW laser power is 142 W, the plastic strain of LALPF increase in laser shock surface, and negative plastic strain in the back surface, which contribute the moment for bending the workpiece.
3. From the result of FEM, the arc height of workpiece is creasing with the power of CW laser power. When the laser power great than 104 W, the increase of arc height becomes faster.

References

[1] Y. Hu, M. Luo, and Z. Yao, "Increasing the capability of laser peen forming to bend titanium alloy sheets with laser-assisted local heating," *Materials & Design,* vol. 90, pp. 364-372, 1/15/ 2016.

[2] A. Mohammadi, H. Vanhove, A. Van Bael, and J. R. Duflou, "Towards accuracy improvement in single point incremental forming of shallow parts formed under laser assisted conditions," *International Journal of Material Forming,* journal article vol. 9, no. 3, pp. 339-351, 2016.

[3] H. Ding, N. Shen, and Y. C. Shin, "Thermal and mechanical modeling analysis of laser-assisted micro-milling of difficult-to-machine alloys," *Journal of Materials Processing Technology,* vol. 212, no. 3, pp. 601-613, 2012.

[4] J. Widłaszewski, "Analysis of deformations induced by a laser beam pulse," in *International Workshop on Thermal Forming and Welding Distortion*, 2008.

[5] G. Germain, F. Morel, J.-L. Lebrun, and A. Morel, "Machinability and Surface Integrity for a Bearing Steel and a Titanium Alloy in Laser Assisted Machining," *Lasers in Engineering (Old City Publishing),* vol. 17, 2007.

[6] J. Yang, S. Sun, M. Brandt, and W. Yan, "Experimental investigation and 3D finite element prediction of the heat affected zone during laser assisted machining of Ti6Al4V alloy," *Journal of Materials Processing Technology,* vol. 210, no. 15, pp. 2215-2222, 11/19/ 2010.

[7] H.-S. Shen, "Nonlinear bending response of functionally graded plates subjected to transverse loads and in thermal environments," *International Journal of Mechanical Sciences,* vol. 44, no. 3, pp. 561-584, 3// 2002.

[8] H. Meyer and D. S. Kleponis, "An analysis of parameters for the johnson-cook model for 2-inch thick rolled homogeneous armor," *Simulation Series,* vol. 30, pp. 12-17, 1998.

[9] Y. Hu and R. V. Grandhi, "Efficient numerical prediction of residual stress and deformation for large-scale laser shock processing using the eigenstrain methodology," *Surface and Coatings Technology,* vol. 206, no. 15, pp. 3374-3385, 3/25/ 2012.

[10] Y. Hu, Y. Han, Z. Yao, and J. Hu, "Three-Dimensional Numerical Simulation and Experimental Study of Sheet Metal Bending by Laser Peen Forming," *Journal of Manufacturing Science and Engineering,* vol. 132, no. 6, pp. 061001-061001, 2010.

[11] W. Zhang, Y. L. Yao, and I. C. Noyan, "Microscale Laser Shock Peening of Thin Films, Part 1: Experiment, Modeling and Simulation," *Journal of Manufacturing Science and Engineering,* vol. 126, no. 1, pp. 10-17, 2004.

[12] L. Berthe, R. Fabbro, P. Peyre, L. Tollier, and E. Bartnicki, "Shock waves from a water-confined laser-generated plasma," *Journal of Applied Physics,* vol. 82, no. 6, pp. 2826-2832, 1997.